8.1 INFLUENCE OF MASS ON DISPLACEMENT THRESHOLD—W. Setyawan, A. P. Selby, G. Nandipati, K. J. Roche, R.J. Kurtz (Pacific Northwest National Laboratory, Richland, WA 99352) and B. D. Wirth (University of Tennessee, Knoxville, TN 37996)

OBJECTIVE

The objective of this research is to investigate how displacement threshold energy changes with atomic mass for the same interatomic potential.

SUMMARY

Molecular dynamics simulations are performed to investigate the effect of mass on displacement threshold energy in Cr, Mo, Fe and W. For each interatomic potential, the mass of the atoms is varied among those metals for a total of 16 combinations. The average threshold energy over all crystal directions is calculated within the irreducible crystal directions using appropriate weighting factors. The weighting factors account for the different number of equivalent directions among the grid points and the different solid angle coverage of each grid point. The grid points are constructed with a Miller index increment of 1/24 for a total of 325 points. For each direction, 10 simulations each with a different primary-knock-on atom are performed. The results show that for each interatomic potential, the average threshold energy is insensitive to the mass; i.e., the values are the same within the standard error. In the future, the effect of mass on high-energy cascades for a given interatomic potential will be investigated.

PROGRESS AND STATUS

Introduction

We have started to explore displacement cascade morphologies and their implications on defect creation and defect clustering by simulating cascades in W as a function of the kinetic energy of the primary knock-on atom (PKA). In our previous report [1], it was found that the dependence of the number of surviving Frenkel pairs (N_{FP}) on the PKA energy (E), exhibits three different characteristic domains presumably related to the different cascade morphologies that form. In the sub-threshold regime with E < 0.2 keV (region 1), the cascade is characterized by a hit-or-miss type of Frenkel pair (FP) production near the displacement threshold energy (E_d). For E in the range of 0.3 – 30 keV (region 2), the defect production curve exhibits a sublinear dependence, $N_{FP} \sim E^{0.74}$, associated with a compact cascade morphology. For E > 30 keV (region 3), the cascade morphology consists of complex branches or interconnected damage regions. In this interconnected morphology, large interstitial clusters form from superposition of interstitials from nearby damage regions. In this regime, a superlinear dependence is observed, $N_{FP} \sim E^{1.36}$. On a log-log scale, one may determine the intersection of the fit lines of region 2 and region 3. The PKA energy at this intersection is defined as the transition energy. It is expected that the transition energy is higher for higher E_d. The exact relation is still under investigation. In addition, E_d may not be the only factor determining the transition energy. Mass may also play a role. In this report, we firstly investigate how changing the mass affects the threshold energy itself within the same interatomic potential. In this report, the results for Cr, Fe, Mo and W are presented.

Simulation Details

The molecular dynamics (MD) technique is employed to calculate the threshold energy. The MD simulations are performed using the LAMMPS code [2]. The interatomic forces are derived mostly from Finnis-Sinclair (FS) potentials [3] which have been modified and extended for cascade simulations; Fe by Calder et al. [4], Mo by Salonen et al. [5, 6] and W by Juslin et al. [6, 7]. For Cr, the FS potential developed by Bonny et al. is employed [8] with the short-range extension done by Juslin.

Periodic boundary conditions are applied along all axis coordinates. We use an orthorhombic box of 20×18×16 supercells (along x, y, and z, respectively) to avoid the self-interaction of the SIA moving along

the <111> directions due to the periodic boundaries. The box contains 11,520 atoms. In test runs using 10 PKAs in each direction of [100], [110], [111], and [136], a smaller box size of 18×16×14 is used and the results are the same within the standard error as with the 20×18×16, giving a confidence that the 20×18×16 box is sufficient. We have also verified visually that replacement events are contained within the box when an SIA is created. Before a displacement is initiated, the system is equilibrated at 10 K and zero pressure for 20 ps with a Nosé-Hoover thermostat with a 1-ps time constant.

For the displacement simulations, a border region is defined with two atomic layers as shown in Figure 1 (black atoms). Note that due to the periodic boundaries, the border region would completely enclose the active region (gray atoms). The simulation cell shape and volume are fixed at the value obtained from the equilibration run. The atoms in the active region are evolved in a microcanonical (*NVE)* ensemble. A Nosé-Hoover thermostat at 10 K with a time constant of 0.1 ps is applied to the atoms in the border region to model the heat extraction. From visualization, it is evident that a 3 ps run is appropriate for observing defect creation. Therefore, the simulation is followed up to 3 ps with 1-fs time step. In the test runs as described previously, we have also verified that simulations up to 5 ps give the same results.

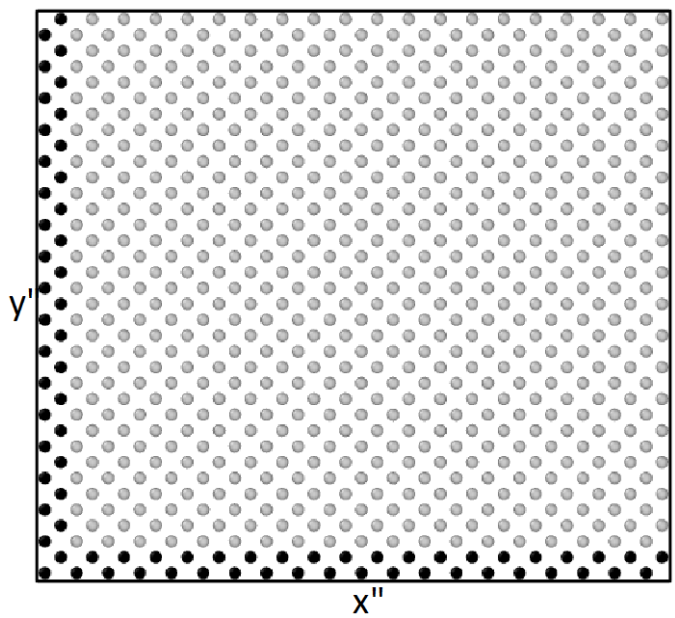

Figure 1. Setup of the simulation cell for the displacement simulations constructed from 20×18×16 supercells along x, y and z respectively. The box contains 11,520 atoms. Border atoms are plotted in black and thermostated at 10 K to model heat extraction. Periodic boundaries are applied in all axes.

The average displacement threshold energy is defined as

$$E_d = \frac{1}{4\pi}\int_0^{4\pi} E_d(\Omega)d\Omega. \quad (1)$$

From a point symmetry consideration, the average E_d can be calculated within the set of irreducible crystal directions (ICD). The ICD and the PKA direction grid used in this study are shown in Figure 2a. If the ICD is employed, it is necessary to account for the different multiplicity of each grid point to correctly calculate the average. The multiplicity represents the number of equivalent directions of a grid point. In Figure 2b, the multiplicity of each point is shown as the number following the x character within the parentheses. The grids are constructed with a Miller index increment of 1/24 resulting in a total of 325 points. Note that these points are not located on the surface of a sphere centered at the origin. Therefore, an appropriate weight due to the different solid angle of each point needs to be taken into account. The

solid angle of point-i, $\Delta\Omega_i$, is calculated as the solid angle enclosing a small sphere with a diameter D = 1/24 (i.e. the sphere fits in to each grid) centered at grid point-i, as illustrated in Figure 2a. Finally, Equation 1 becomes

$$E_d = \sum_i E_{d,i} P_i \Delta\Omega_i / \sum_i P_i \Delta\Omega_i \tag{2}$$

$$\Delta\Omega_i(h,k,l) = 2\pi\left(1 - \frac{\sqrt{h^2+k^2+l^2}}{\sqrt{h^2+k^2+l^2+D^2/4}}\right) \tag{3}$$

where P_i denotes the number of equivalent directions for grid point-i.

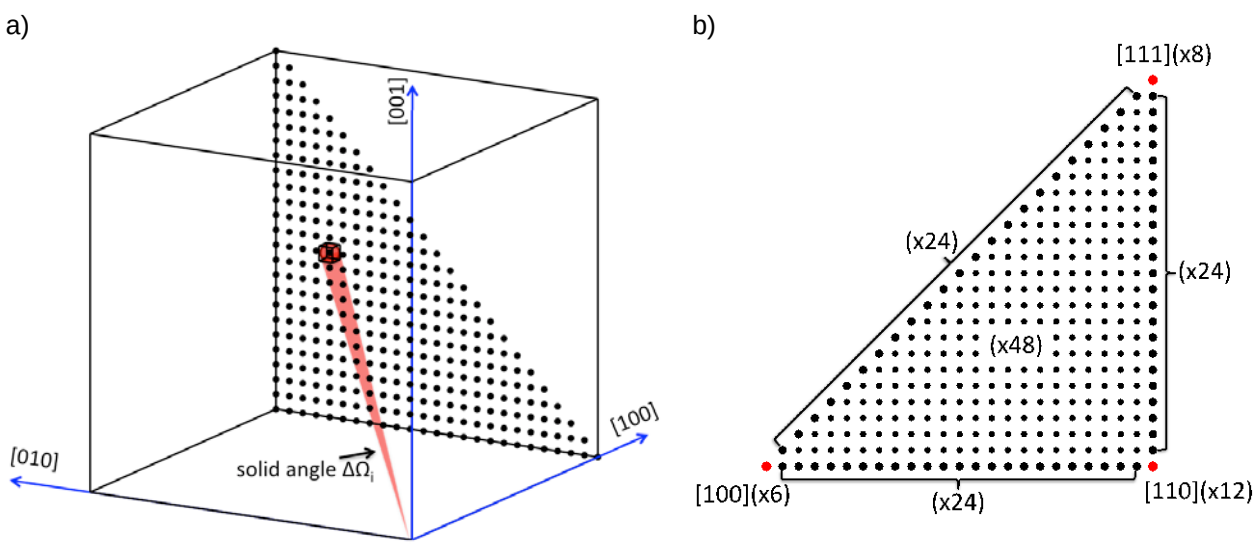

Figure 2. a) The irreducible part of the crystal directions and the grid points for the PKA directions. The grids are constructed with a Miller index increment of 1/24 resulting in a total of 325 points. b) The number of equivalent directions of each point is shown as the number following the x character within the parentheses.

Results

For each direction, the threshold energy is averaged over 10 simulations using a different PKA chosen near the center of the box. To search for the threshold energy, the PKA energy is incremented by 5 eV until a defect is detected, then decremented by 1 eV until no defects are detected. The threshold energy for a specific simulation is taken to be the minimum energy where a defect is created. Wigner-Seitz cell occupancy is used to recognize defect creation. The average threshold energy calculated with Equation 2 for all combinations of masses and interatomic potentials used in this study is presented in Table 1. For each interatomic potential, the results show that the displacement threshold energy is insensitive to mass, i.e. the values are the same within the standard error. In the future, the effect of mass on high-energy cascades for a given interatomic potential will be investigated. In high-energy cascades, the mass is expected to play a more important role than in sub-threshold displacement events due to the larger volume of material involved affected by cascade damage.

Table 1. Calculated average of the displacement threshold energy, in eV, as a function of interatomic potential (row-wise) and mass (column-wise). The mass is given in parentheses. Standard error of the threshold energy is included.

	Cr (52.00)	Fe (55.85)	Mo (95.94)	W (183.85)
Cr potential	34.4 ± 1.5	33.4 ± 1.5	34.0 ± 1.5	33.8 ± 1.4
Fe potential	41.4 ± 1.6	41.8 ± 1.6	41.8 ± 1.7	41.3 ± 1.3
Mo potential	78.6 ± 2.8	77.4 ± 2.9	78.7 ± 2.9	77.9 ± 2.9
W potential	123.6 ± 4.4	123.7 ± 4.2	122.7 ± 4.1	122.6 ± 4.4

We would like to acknowledge the contributions from N. Juslin in improving the short-range of the Cr potential [8]. Computations were performed on Olympus supercomputer (FUSION account) at Pacific Northwest National Laboratory.

REFERENCES

[1] W. Setyawan, et al., Fusion Reactor Materials Program Semiannual Report 54 (2013) 201.
[2] S. Plimpton, J. Comp. Phys., 117, (1995), 1.
[3] M. W. Finnis and J. E. Sinclair, Phil. Mag. A 50, (1984), 45.
[4] A. F. Calder and D. J. Bacon, J. Nucl. Mater., 207, (1993), 25.
[5] E. Salonen, T. Järvi, K. Nordlund and J. Keinonen, J. Phys. Cond. Mat., 15, (2003), 5845.
[6] G.J. Ackland and T. Thetford, Phil. Mag. A 56, (1987), 15.
[7] N. Juslin and B.D. Wirth, J. Nucl. Mater., 432, (2013), 61.
[8] G. Bonny, R. C. Pasianot, D. Terentyev, and L. Malerba, Phil. Mag. 91, (2011), 1724.